

Mass-independent isotope effect in the earliest processed solids in the solar system: A possible chemical mechanism

R. A. Marcus

Noyes Laboratory of Chemical Physics, California Institute of Technology, Pasadena, California 91124

(Received 8 July 2004; accepted 12 August 2004)

A major constraint is described for a possible chemical origin for the “mass-independent” oxygen isotope phenomenon in calcium-aluminum rich inclusions (CAIs) in meteorites at high temperatures (~ 1500 – 2000 K). A symmetry-based dynamical η effect is postulated for O atom-monoxide recombination on the surface of growing CAIs. It is the surface analog of the volume-based η effect occurring in a similar phenomenon for ozone in the gas phase [Y. Q. Gao, W. C. Chen, and R. A. Marcus, *J. Chem. Phys.* **117**, 1536 (2002), and references cited therein]: In the growth of CAI grains an equilibrium is postulated between adsorbed species $XO(ads) + O(ads) \rightleftharpoons XO_2^*(ads)$, where $XO_2^*(ads)$ is a vibrationally excited adsorbed dioxide molecule and X can be Si, Al, Ti, or other metals and can be C for minerals less refractory than the CAIs. The surface of a growing grain has an entropic effect of many order of magnitude on the position of this monoxide-dioxide equilibrium relative to its volume-based position by acting as a concentrator. The volume-based η effect for ozone in the earlier study is not applicable to gas phase precursors of CAIs, due to the rarity of three-body recombination collisions at very low pressures and because of the high H_2 and H concentration in solar gas, which reduces gaseous O and gaseous dioxides and prevents the latter from acting as storage reservoirs for the two heavier oxygen isotopes. A surface η effect yields $XO_2^*(ads)$ that is mass-independently rich in ^{17}O and ^{18}O , and yields $XO(ads) + O(ads)$ that is mass-independently poor in the two heavier oxygen isotopes. When the $XO_2^*(ads)$ is deactivated by vibrational energy loss to the grain, it has only one subsequent fate, evaporation, and so undergoes no further isotopic fractionation. After evaporation the XO_2 again has only one fate, which is to react rapidly with H and ultimately form ^{16}O -poor H_2O . The other species, $O(ads) + XO(ads)$, are ^{16}O rich and react with $Ca(ads)$ and other adsorbed metal atoms or metallic monoxides to form CAIs. The latter are thereby mass-independently poor in ^{17}O and ^{18}O . Some $O(ads)$ used to form the minerals are necessarily in excess of the $XO(ads)$, because of the stoichiometry of the mineral, and modify the fractionation pattern. This effect is incorporated into the mechanistic and mathematical scheme. A merit of this chemical mechanism for the oxygen isotope anomaly is that only one oxygen reservoir is required in the solar nebula. It also does not require a sequestering of intermediate products which could undergo isotopic exchange, hence undoing the original isotopic fractionations. The gas phase source of adsorbed O atoms in this environment is either O or H_2O . As inferred from data on the evaporation of Mg_2SiO_4 taken as an example, the source of $O(ads)$ is primarily H_2O rather than O and is accompanied by the evolution of H_2 . Nonisotopic kinetic experiments can determine more sharply the mechanism of condensed phase growth of these minerals. Laboratory tests are proposed to test the existence of a surface η effect on the growing CAI surfaces at these high temperatures. © 2004 American Institute of Physics. [DOI: 10.1063/1.1803507]

I. INTRODUCTION

The earliest processed solids in the solar system, the calcium-aluminum rich inclusions (CAIs) in chondritic meteorites, are about 4.56×10^9 years old.^{1–5} The CAIs show a “mass-independent” oxygen isotope effect, namely, an equal deficiency in the heavy isotopes ^{17}O and ^{18}O relative to the mean isotopic composition of ocean water: The slope of a plot of $(^{17}O/^{16}O)_{\text{sample}} / (^{17}O/^{16}O)_{\text{standard}}$ versus the corresponding quantity for ^{18}O is close to 1.0, instead of having the usual and well understood mass-dependent value close to 0.52.

This unexpected mass-independent phenomenon, whose origin remains unknown some 30 years after its striking dis-

covery by Clayton *et al.*,⁶ has been the subject of numerous studies, e.g., Refs. 7–21. The phenomenon is also observed in chondrules,¹⁹ a much more extensive component of chondrites, and frequently regarded as forming slightly later than CAIs. The interest lies in what clues this unusual isotopic effect and other data^{22–41} can provide about the formation of the solar system. Some nonisotopic observations, for example, point to forming most CAIs in environments which vary from more oxidizing to more reducing than that of a solar gas, e.g., Refs. 42 and 43. “Dust enriched” scenarios for the initial composition of the pre-CAI environment are often considered in the literature, e.g., Refs. 37 and 42–47, and are more oxidizing than a solar gas. However, for the

present analysis it is the composition of the adsorbed species on the surface of the growing CAI grains, rather than that in the gas phase, which is important. It is shown in Sec. II B that the two can be very different. For brevity, the growing CAI precursor grains are referred to simply as CAIs in the following (“CAI precursors” since their formation may be followed by subsequent processing such as melting and re-solidification).

If the mass-independent phenomenon has a chemical origin, which is by no means assured, it places constraints on the conditions under which the CAIs are formed. Our aim is to describe kinetic conditions which, if fulfilled, yield a mass-independent formation of CAIs, suggest laboratory tests, and make predictions.

A nucleosynthetic origin of the phenomenon was initially postulated by Clayton.⁶ Fractionation by self-shielding is also a possibility.^{48–50} A chemical origin has been proposed by Thiemens,⁵¹ who discussed various possible reactions. Arguments against the nucleosynthetic proposal include the absence of related isotopic anomalies in the same solids.² A nucleosynthetic galactic evolution model⁵² remains a viable possibility, but presently not testable.⁵³ By far the greatest fractionation due to self-shielding would be between ¹⁶O versus ¹⁷O and ¹⁸O, because of the large difference in abundance.

Optical shielding calculations have been initiated⁵⁴ and may also reveal the extent of optical fractionation between ¹⁷O and ¹⁸O. A detailed analysis of chemical mechanisms remains to be undertaken and is the subject of the present paper.

A chemical mechanism has been documented for the mass-independent isotope effect in ozone formation⁵⁵ in the laboratory and in the stratosphere, e.g., Refs. 56–58. Ozone formed by photolysis^{56–58} or electric discharge⁵⁹ in oxygen is approximately equally enriched in ¹⁷O/¹⁶O and ¹⁸O/¹⁶O. The enrichment at room temperature is about 100 parts per mil relative to the initial composition. An explanation has been given^{60–64} and provides insight into data on many different experiments, including those where there is extensive isotopic exchange,^{55–59} those where there is none,^{65–68} the different pressure effects for each of these conditions,^{68–70} and experiments using oxygen heavily enriched in ¹⁷O and ¹⁸O.^{71–75} We apply the concepts here, particularly the symmetry-based η effect described for ozone in Refs. 60–64.

The physical nature of the η effect is summarized in Appendix A. In the present case ozone is not involved, but the chemical physics of the phenomenon^{60–64} would be similar for any molecule with symmetric and asymmetric isotopologs. For the CAIs, however, we shall see that a surface-based rather than as in ozone a volume-based η effect is required. Laboratory experiments can provide the information on whether or not such an effect exists.

The equal deficiency in ¹⁷O and ¹⁸O in the CAIs is as much as 50 or so per mil for the more refractory minerals.^{7–21} For minerals which have a condensation temperature lower than the CAIs, as in chondrules, this deficiency is typically less, even becoming a slightly positive enrichment.¹⁹ Since the enrichments in the CAIs are

opposite in sign from those in ozone formation, the problem has, in a sense, been “turned on its head.” The CAI minerals are many and, in terms of readily recognizable formula units, they include hibonite $\text{CaO}(\text{Al}_2\text{O}_3)_6$, anorthite $\text{CaO}(\text{Al}_2\text{O}_3)(\text{SiO}_2)_2$, spinel $\text{MgO}(\text{Al}_2\text{O}_3)$, melilite $(\text{CaO})_2(\text{MgO})_x(\text{SiO}_2)_{1+x}(\text{Al}_2\text{O}_3)_{1-x}$, and non-Ca, Al minerals such as forsterite $(\text{MgO})_2\text{SiO}_2$. (In mineralogists’ formulas the more customary designations are $\text{CaAl}_{12}\text{O}_{19}$, $\text{CaAl}_2\text{Si}_2\text{O}_8, \dots$)

A local exhaustion of Al and Ca due to their limited abundance stops the formation of those CAIs. As the temperature falls, ferromagnesian silicates (chondrules) can condense with Fe and Mg as the metallic elements and perhaps with some overlap of the two depositions.

An open question is whether the sequence of minerals in these systems represents largely a condensation or an evaporation sequence. The sequences have been discussed in Refs. 44–47, 76, and 77. Any mechanism should also ultimately explain the different textural properties of the meteoritic components, as well as the presence of elements that form volatile oxides, among other observations.

The system is now much more complex than the ozone system, since many additional species and reaction steps occur. In addition to gas phase reactions there are now also evaporation and mineral-forming condensation. Even the primary act for a possible chemical mechanism is not known.

Laboratory attempts to produce a mass-independent effect of the magnitude experimentally observed in the CAIs have not yet been successful,^{78–80} apart from a single experiment discussed in Sec. III which showed intriguing results. No detailed theory was available to assist in the selection of experimental conditions. In the case of ozone the theory benefited from a large body of experimental data. The existing body of data on the CAIs places constraints on theory, and theoretically based laboratory experiments for forming the CAIs under controlled conditions remain to be undertaken.

The paper is organized as follows: A theory is described in Sec. II containing preliminary remarks on the model (Sec. II A), a description of the key role of the surface in shifting the position of monoxide/dioxide equilibria for adsorbed species (Sec. II B), a summary of the specific constraints imposed by the phenomenon on the theory (Sec. II C), kinetic equations (Sec. II D), and condensation kinetics (Sec. II E). An approximate equation for the resulting mass-independent isotopic enrichment is given by Eqs. (10), (12), and (13). The results are discussed and proposed experiments are given in Sec. III.

II. THEORY

A. Model and assumptions

We assume a system where the mass-independent fractionation is occurring in a high temperature environment (~1500–2000 K) and at low pressures (~0.001 bar). When we made calculations for these conditions we found (Appendixes B and C) that a gas phase η effect that applied to ozone cannot be invoked to explain the same phenomenon for CAIs: At high temperatures in the low pressure H₂-rich environment the “three-body” recombinations, whose analogs

were responsible for the η effect for ozone in gases, cannot compete with two-body reactions such as $O+H_2\rightarrow OH+H$, in determining the steady-state O atom concentration (Appendix B). Nor can chemiluminescent recombination reactions compete, e.g., the rate of the reaction $O+CO\rightarrow CO_2+h\nu$ (Ref. 81) is much less than that of the $O+H_2$ reaction in competing for the O atoms (Appendix B). Equally importantly in the early solar system, gas phase dioxides such as SiO_2 cannot play the same storage role for ^{17}O and ^{18}O that O_3 did in the atmospheric system. They are too unstable in the high temperature H_2 -rich environment to serve in that capacity (Appendix C and Ref. 82).

Surface recombination on grains instead of in the gas phase has frequently been invoked for chemical reactions at low pressures, notably for $2H\rightarrow H_2$ and others.⁸³ The many orders of magnitude entropic effect of a surface on the local (surface) position of dioxide/monoxide equilibria is shown in Sec. II B. The entropic effect acts by providing a locally high concentration of species on the surface, in contrast with the dilute concentration in the gas phase, thus shifting the position of an equilibrium of the $A+B\rightleftharpoons C$ type to the right. Although the probability of collision of atoms and molecules with the surface to provide this surface concentration is small (estimates are given in Appendix D), such collisions are needed in any case for the growth of a condensed phase, whether it is a solid or a melt. So this way of concentrating atoms and molecules, and so favoring a shift towards C in the recombination of A and B , is not an added penalty to the overall condensation process.

Since recombinations in the gas phase are too rare to provide a viable mechanism for the formation of CAI precursor molecules, any invocation of an η effect in recombination reactions leading to a CAI must therefore be for reactions occurring on the CAI surface. In this context, we shall see that there is a profound mechanistic difference between the role of the surface in the present case and that found in ozone formation. In the latter, the mass-independent effect disappeared when the recombination occurred on the walls of the reaction vessel,⁶⁹ due to diffusion control or a wall-induced deactivation of the vibrationally excited intermediate.

B. Role of surface in shifting XO_2/XO and AlO/Al equilibria

We proceed to estimate the entropic surface effect on the reaction $XO+O\rightleftharpoons XO_2$, where X is Si or Al, in the case of CAI precursors. Similar remarks apply to $Al+O\rightleftharpoons AlO$. The entropic effect on this equilibrium is seen below to be some 12 or so orders of magnitude, though modified by an energy effect.

In the catalytic properties of surfaces one factor is entropic, the ability of these surfaces to bring the reactants to a high local concentration. Their ability to do so depends on forming physical or chemical bonds with the atoms and the molecules. The position of the $A+B\rightleftharpoons C$ equilibrium on the surface can be very different from that in the gas phase. For example, at 2000 K, the ratio of SiO_2/SiO is 3.3×10^{-6} in solar gas and the concentration of O is $\sim 4\times 10^8\text{ cm}^{-3}$.⁸² We compare this result with the equilibrium on a grain surface.

For concreteness, we suppose that one O is adsorbed every 10^4 \AA^2 of grain surface. The local surface O concentration is then 10^{-4} \AA^{-2} . Again, apart from energetic concerns, if in a ‘‘back of the envelope’’ estimate the O is considered to have an order of magnitude amplitude of motion $\sim 1\text{ \AA}$ normal to the surface (a large estimate, to be conservative), its local ‘‘concentration’’ becomes $10^{21}\text{ atoms cm}^{-3}$, an increase of a factor 2.5×10^{12} . The gas phase value⁸² for $SiO_2/SiO\sim 2\times 10^{-6}$ is shifted entropically by this large factor. However, an energy term, ΔE in Eq. (3) below, will reduce this enhancement, since SiO and O are expected to be more strongly adsorbed on the surface than SiO_2 .

A more formal analysis is obtained in a standard way, treating, for simplicity, the motion parallel to the surface as free. We denote O, XO, and XO_2 by A , B , and C , respectively, and write the gas phase concentrations in terms of partition functions,

$$\frac{C}{A\cdot B} = \frac{h^3}{(2\pi\mu kT)^{3/2}} \frac{q_C}{q_{AB}} e^{-\Delta E/kT}, \quad (1)$$

where μ is the reduced mass of XO and O, and q_C and q_{AB} are the rotational-vibrational partition functions of the C and the AB pair, respectively, in the gas phase. For species all adsorbed on the surface, we have

$$\frac{C_{ads}}{A_{ads}\cdot B_{ads}} \cong \frac{h^2}{2\pi\mu kT} \frac{h\nu}{kT} \frac{q_C}{q_{AB}} e^{-\Delta E_{ads}/kT}, \quad (2)$$

where ν is a typical vibration frequency of the adsorbed species for motion normal to the surface and ΔE_{ads} is the dissociation energy for the surface reaction. We take q_C and q_{AB} to be roughly the same as in Eq. (1) to obtain a rough estimate. We then find that

$$\frac{(XO_2)_{ads}/(XO)_{ads}}{XO_2/XO} = \frac{kT}{\nu} \frac{1}{\sqrt{2\pi\mu kT}} \frac{O_{ads}}{O} e^{-(\Delta E_{ads}-\Delta E)/kT}. \quad (3)$$

Introducing the cited values of O_{ads} and O and taking $\nu\sim 100\text{ cm}^{-1}$ and μ as the reduced mass for the (XO,O) pair with $X=Si$, the preexponential factor in Eq. (3) is 6×10^{11} . This value is close to the rough estimate of 2.5×10^{12} given above. The gas phase XO_2/XO ratio of 2×10^{-6} for SiO_2/SiO and an approximately similar value for $X=Al$ show that the XO_2/XO ratio is shifted dramatically from its gas phase value, apart from the effect of the surface on the dissociation energy of the reaction, the $\Delta E_{ads}-\Delta E$ in exponent in Eq. (3). Analogous remarks on enhancement also apply to the AlO/Al ratio. Had a localized site model been used for the adsorbed molecules instead of a mobile phase, the right-hand side of Eq. (2) would have been even larger and the adsorbed ratio larger than that in Eq. (3).

At 1500 K the SiO_2/SiO ratio⁸² is $\sim 6\times 10^{-7}$, i.e., factor of 3 less than the value at 2000 K. The O concentration is $\sim 3\times 10^3\text{ atoms cm}^{-3}$, about five orders of magnitude less than the value at 1600 K. So now the entropic effect is even larger than at 2000 K, but again is modified by the energy term in Eq. (3). A quasiequilibrium constant given later for reaction (17) will have the same value, regardless of whether the O_{ads} is deposited by O or H_2O .

Competing Processes on Surface

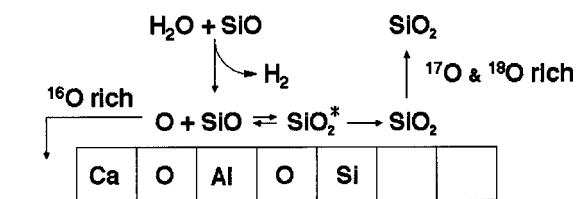


FIG. 1. Schematic diagram of competing processes on the surface of a growing CAI mineral. In more oxidative environments, the initial step could occur as $O + SiO \rightarrow O_{ads} + SiO_{ads}$.

C. Specific constraints

We first recall some relevant abundances in CI chondrites,^{84,85} since these abundances and their relevant chemical speciation play a key role in any theory. As an atomic fraction of the Si abundance, Al and Ca are very small, 0.08 and 0.06, respectively, while O, C, Mg, and Fe are 8, 0.8, 1, and 0.9 times that of Si, respectively.^{84,85} The CAI minerals form less than 5% of the total solids in the chondrites.³³

With the arguments in the preceding section in mind, we consider the following constraints:

(1) We consider CAIs for which the mass-independent phenomenon derives from condensation rather than evaporation. We leave open the question of whether there may also be a similar η effect for evaporation.

(2) A surface-adapted η effect occurs for the recombination of O atoms and monoxides on a CAI surface. [The adsorbed oxygen atoms O_{ads} can arise from a surface reaction, $H_2O(g) + \text{surface} \rightarrow H_2(g) + O_{ads}\text{-surface}$, or from gas phase O atoms. The η effect itself is independent of the source of O_{ads} .]

(3) The CAIs are formed from adsorbed O atoms and monoxides rather than from adsorbed dioxides and polyoxides. The recombination on the surface to form dioxides in point (2) competes with incorporation of the adsorbed O, monoxides, Ca, Al, Mg, and other adsorbed species into the growing CAI.

(4) Dioxide formed by surface recombination in point (2) largely evaporates, as in Fig. 1. In the vapor phase it quickly reacts chemically with H, producing a heavy isotope enriched reservoir.

The mechanism in points (1)–(4) is depicted in Fig. 1. Condition (2) introduces the mass-independent property of O atom-monoxide recombination in a form where it occurs on the CAI surface. Condition (3) ensures that the η effect for CAI formation leads to ^{16}O -rich rather than to ^{16}O -poor CAIs. A consequence of the η effect is to produce a dioxide equally enriched in ^{17}O and ^{18}O .^{60–64} Point (4) notes the fate of the dioxides after they evaporate. When the dioxides XO_2 and XOQ formed in reactions (4)–(6) evaporate, as in Fig. 1, they are quickly reduced by H to form OH and QH (Appendix C). This OH and QH then react readily with H_2 to form ^{17}O and ^{18}O enriched H_2O (Appendix E).

There is experimental evidence for condition (3) from

studies of the species formed the reverse reaction,⁸⁶ the evaporation of Mg_2SiO_4 . Using a free evaporation configuration (“Langmuir,” nonequilibrium)⁸⁶ it was deduced that the dissociation of Mg_2SiO_4 is into SiO and O, and not directly into SiO_2 . By condition (3), this mechanism is assumed for the reverse reaction, the condensation.

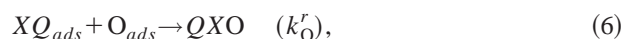
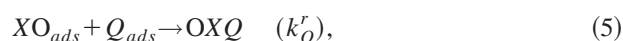
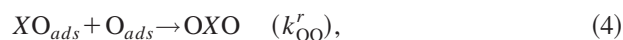
Isotopic exchange occurs readily in the gas phase between O atoms and diatomic molecules when there is no energy barrier to forming the triatomic complex. In cases of common interest there is not, e.g., for ozone.^{60–64} This isotopic exchange does not require a “third-body” and does not interfere with mass independence.⁶⁰ In fact, paradoxically perhaps, the isotopic exchange is needed for mass independence (Appendix A and Ref. 60). Isotopic exchange may also occur on the surface, but it certainly occurs in the gas phase.

H_2O is calculated in Sec. IID to be a more important source of O_{ads} than O under the existing conditions. For the case that $O \rightarrow O_{ads}$ is the preferred source, it would be for minerals formed in some highly oxidative environment. It is reasoned in Appendix D that there is an adequately maintained thermal concentration of gas phase O atoms at 1500–2000 K sufficient to avoid depletion by the formation of the CAIs. Nevertheless, nonthermal sources may provide an enhanced concentration of atoms and radicals as well as raise the temperature of the system.

The ^{17}O and ^{18}O enrichment of H_2O arising in point (4) has very little initial effect on the isotopic composition of H_2O , since the O content in CAIs is only a small fraction of that in the total H_2O . However, after a large amount of other minerals has formed this ^{17}O and ^{18}O enrichment has an accumulative effect on the H_2O isotopic composition.

D. Kinetic equations

We denote the monoxides by XO , where X is Si, Al, and others. X can also be C, but the C oxides are too volatile to form CAIs. The rates of the unsuccessful reactions, i.e., those pairs which do not form CAIs but lead to gaseous dioxides that are reconverted to monoxides, are given by reactions (4)–(6):



where “ads” denotes adsorbed species and the k^r s denote recombination rate constants on the surface. K is the equilibrium constant isotopic exchange reaction (7) for the gas phase or adsorbed phase. Q denotes ^{17}O or ^{18}O , and the η effect is contained in the k^r s for reactions (4)–(6), which together with reaction (7) occur via vibrationally excited molecules XO_2^* .^{60–64} Their properties lead to the η effect (Appendix A).

To derive a theoretical expression for the k^r s in Eqs. (4)–(6), we let the rate of formation of XO_2^* on the surface in the energy range $(E, E+dE)$ be $k_f XO \cdot O dE$, where X is Si in the illustrative example in Fig. 1 and k_f depends upon E . The rate of the reverse reaction, the dissociation of XO_2^* into

$XO + O$, is written as $k_d XO_2^*$, where k_d again depends upon E . The rate of vibrational energy loss from XO_2^* to the underlying mineral surface, such that the XO_2 can no longer redissociate into $XO + O$, is denoted by $k_c XO_2^*$. This XO_2 ultimately evaporates, as in Fig. 1. In a steady-state approximation for XO_2^* , its concentration is $(k_f/k_c)/(1+k_c/k_d) \times (dE) XO \cdot O$. The k_{OO}^r in Eq. (4) is, after integration over E ,

$$k_{OO}^r = \int k_c(k_f/k_d)/(1+k_c/k_d)dE. \quad (8)$$

This equation is the surface analog of Eq. (1.2) in Ref. 60. However, a fundamental difference in the phenomena to which we alluded earlier is that the successful reactions in the ozone system, successful in that they form ozone, are the unsuccessful reactions here, unsuccessful in that they yield dioxides instead of CAIs. The intramolecular η effect affects in the density of states $\rho(E)$ of the vibrationally excited XO_2^* . The k_d in Eq. (8) is inversely proportional to ρ in RRKM (Rice–Ramsperger–Kassel–Marcus) theory and in this η -modified RRKM theory. So the η effect decreases when k_c/k_d in the denominator in Eq. (8) becomes large, and k_d then cancels. (In physical terms, k^r no longer depends on ρ .) The high thermal energy at 1500–2000 K enhances k_d , compared with its value at room temperature, and so this XO_2^* molecule is expected to be very short lived. An equation similar to Eq. (8) is obtained for k_Q^r and another for k_O^r , when the appropriate k_{fS} and k_{dS} are introduced. These equations are the analogs of Eq. (1.5) in Ref. 60.

In the case of ozone the enrichment decreases with increasing pressure,⁶⁷ since the dependence of k^r on ρ in the equation decreases. However, k^r remains mass independent even after it decreases in magnitude by a factor of 10.⁶⁷ The analog in Eq. (8) of this pressure effect is that the enrichment in the evaporated dioxides decreases with increasing k_c/k_d , but continues to be mass independent, even when this quantity becomes large (factor of 10). Eventually this η effect becomes comparable in magnitude with ordinary mass-dependent effects.⁸⁷ Thus, if SiO_2^* survives for a number of vibrations before redissociation, a surface based η effect becomes possible.

The rate of disappearance of the sum of O and XO on the surface by reaction (4) is $2k_{OO}^r O \cdot XO$. The rate of disappearance of the sum of Q and XQ on the surface by reactions (5) and (6) is $(k_Q^r + k_O^r K) O \cdot XQ$. The rates of formation of the total O content and the Q content on the surface before fractionation will be taken as proportional to the total isotopic O and Q content of the gas, O_T and Q_T , respectively.

For simplicity and notational brevity, we focus on a single X. Denoting a proportionality constant by I , we have for a steady state of the sums (O+XO) and (Q+XQ) on the surface, $IO_T = 2k_{OO}^r O \cdot XO$ and $IQ_T = (k_O^r + k_Q^r K) O \cdot XQ$. The K in Eq. (7) equals unity to about 1 part per mil at the prevailing temperatures.⁸² We then have

$$\left(\frac{Q}{Q_T}\right) / \left(\frac{O}{O_T}\right) = \frac{1}{R}, \quad (9)$$

where Q and O refer to the adsorbed species and

$$R = \frac{k_O^r + k_Q^r K}{2k_{OO}^r}. \quad (10)$$

The K is retained in Eq. (10) even though it is in effect unity, to note the similarity to Ref. 60. In a purely statistical case, it can be shown that $R = 1$, and then there is no fractionation in Eq. (9). Since R exceeds 1, as in Refs. 60–64, the Q/O content on the surface leads to CAIs whose Q/O ratio is less than that in the system as a whole.

We denote the Q and O content in the CAIs by Q_{CAI} and O_{CAI} and treat their ratio as proportional to the steady-state ratio of Q and O contents on the surface. This ratio is less than that in the gas phase, when a surface-based η effect occurs. The individual “rate constant” for each deposition will depend on the various other concentrations such as Ca and Al, but cancel in the ratio of rates. The enrichment in Q, δQ , in the condensate can be defined as the ratio of Q_{CAI}/Q_T , divided by O_{CAI}/O_T , minus 1, and multiplied by 1000. We have

$$\frac{\delta Q}{1000} = \frac{Q_{CAI}/O_{CAI}}{Q_T/O_T} - 1. \quad (11)$$

On statistical grounds the Q_{CAI}/O_{CAI} in Eq. (11) is taken to be equal to the total Q-containing species adsorbed on the surface divided by the total of the O-containing species on the surface. To apply Eq. (11) we need to take into account that in the mineral the O typically exceeds the SiO because of the metallic elements present. So a fraction w of the O in the adsorbed O_{ads} and SiO_{ads} undergoes reactions (4)–(6) and so yields an isotopic ratio given by the $1/R$ in Eq. (9), while a fraction $1-w$ does not and contributes 1 instead of $1/R$. w is the $2SiO/O$ ratio in the mineral. The Q/O content in the mineral relative to that in the entire system is seen to be $(w/R) + 1 - w$, and Eq. (11) then yields

$$\frac{\delta Q}{1000} = \left(\frac{1}{R} - 1\right)w. \quad (12)$$

The right-hand side vanishes when $R = 1$ or $w = 0$, as it should.

The magnitude of w is immediately evident when the mineral contains no Al: We denote the number of formula units of SiO_2 in the mineral by M and the total number of O atoms by $2M + N$. From the definition of w we have

$$w = \frac{2M}{2M + N}. \quad (13)$$

For example, for forsterite, Mg_2SiO_4 , $M = 1$, $N = 2$, and so $w = 1/2$.

To include Al_2O_3 -bearing minerals, we use the following argument based on an interpretation of solid solutions. The formula unit Al_2O_3 replaces groups such as $MgSiO_3$, $CaSiO_3$, and $FeSiO_3$ in a solid solution. On this basis, each Al_2O_3 is equivalent to one SiO_2 and one additional O, i.e., it is assumed to contribute 1 to the value of M and 1 to the value of N . Accordingly, for spinel, $MgAl_2O_4$, we have $M = 1$, $N = 2$, and so $w = 1/2$. For hibonite, $MgAl_{12}O_{19}$, we have $M = 6$, $N = 7$, and so $w = 12/19$. For forsterite, Mg_2SiO_4 , as noted above, $M = 1$, $N = 2$, and so $w = 1/2$; me-

illite, $\text{Ca}_2\text{Mg}_x\text{Si}_{1+x}\text{Al}_{2-2x}\text{O}_7$, has $M=2$, $N=3$, and so $w=4/7$; and pyroxene, $\text{Ca}_y\text{Mg}_{x-y}\text{Fe}_{1-x}\text{SiO}_3$, has $M=1$, $N=1$, and so $w=2/3$. The w 's in these examples vary from $1/2$ to $2/3$, which is not a very large variation.

Although AlO_2 and SiO_2 have very different stabilities with respect to complete dissociation into atoms, their dissociation energies to the monoxides $\text{AlO}_2 \rightarrow \text{AlO} + \text{O}$ and $\text{SiO}_2 \rightarrow \text{SiO} + \text{O}$ are calculated to be essentially the same.⁸² The calculated vibration frequencies of the two molecules are not very different from each other,⁸² those of AlO_2 being smaller. Accordingly, if the surface-based η effect exists, it may be somewhat similar for the surface-adsorbed AlO_2 and SiO_2 species.

The CAI formation is a small conversion (a few percent or less) of the total material and its rate of formation is estimated in Appendix D to be small compared with the rates of any competing gas phase reactions which determine the steady-state O and Q concentrations in the gas phase. Thus, we do not need to take into account the changing gas phase concentrations.

When several minerals are codepositing a detailed mechanistic description of the condensation is ultimately needed for any analysis, but, the main direction is clear, a mass-independent equation is obtained with the deposited minerals being richer in ^{16}O when a surface-based η effect exists.

E. Kinetics of condensation and evaporation

The rate of growth of simple and multicomponent crystals from solution is frequently expressed as a function of $(S-1)$, where S is the supersaturation.⁸⁸⁻⁹¹ The behavior is often interpreted in terms of the spiral dislocation theory of crystal growth.⁹¹ However, the concentrations used in such studies are usually stoichiometric. More generally, the rate depends also on ionic ratios.⁹² We use instead a different analysis in the literature, typically applied to evaporation of solids (Ref. 93 and references cited therein), but also applicable to condensation of vapors [it is designated as HKS (Hertz-Knudsen-stoichiometric fluxes) below]. While it is less mechanistic, in that it introduces a parameter α , it has the merit of introducing in a simple way the correct ratios of the fluxes of the depositing species. The two approaches have the same dependence on concentrations only in the linear $(S-1)$ regime and then only when the concentrations are proportional to their equilibrium values. (In most solution crystallization experiments the rate is quadratic in $S-1$, the extra factor being due to the dependence of a "kink" density on $S-1$ in spiral growth theory when $S-1$ is small.⁸⁸⁻⁹¹)

We consider next some results obtained for vapor-solid equilibria. Here, unlike crystallization from solution there are no or almost no experimental studies of the kinetics of condensation. The study of the reverse process of evaporation has been extensive, particularly for Mg_2SiO_4 , but the concentrations of the congruently evaporating species have usually been fixed by the stoichiometry of the mineral. In detailed condensation studies, in contrast, the concentrations of the condensing species could be varied independently. In the absence of such information we focus on results available

from evaporation. We utilize studies of evaporation of Mg_2SiO_4 (Ref. 93 and references cited therein). The rate of evaporation of various magnesium minerals⁹⁴ has been studied in the presence of the different partial pressures of a product, oxygen that reduces the rate of the evaporation. The results are discussed elsewhere using the HKS formalism.⁹⁵

In the reactions before and following the evaporation of the dioxides in Fig. 1, there is a rapid equilibration of oxygen isotopes and a chemical equilibrium among the species OH , H_2O , O , SiO , and CO : For example, from data on rate constants and estimated⁸² concentrations in the solar gas the lifetimes of OH reacting with H_2 , of OH reacting with H , and of SiO_2 reacting with H are very short (Appendixes C and E). These two-body gas phase reactions provide thereby a rapid gas phase equilibration of their species at 1500–2000 K.

We first consider chemical steps for a condensation using Mg_2SiO_4 purely as an illustration, irrespective of any isotope effect:



or



followed by reactions of Mg_{ads} , SiO_{ads} , and O_{ads} to form Mg_2SiO_4 .

In the HKS method a Hertz-Knudsen-based expression⁹⁶⁻⁹⁸ for the flux density J_i is introduced for each species i :

$$J_i = \alpha_i \sqrt{kT/2\pi m_i} (c_i - c_i^e),$$

where α_i , m_i , c_i , and c_i^e are the collision sticking probability, the mass, the concentration, and the equilibrium concentration of the i th species, respectively. To achieve the desired stoichiometry of the condensed phase, the ratios of fluxes, J_i/J_j , are set equal to the ratio of stoichiometric numbers of the species in the mineral, ν_i/ν_j . Since the product of the equilibrium concentrations $\prod_i (c_i^e)^{\nu_i}$ is known from thermodynamics to be a constant, these equations can be solved for the individual c_i^e 's as a function of all c_j 's. As an approximation, the individual α_i 's are set equal to a constant α , where by experiment $\alpha \sim 0.1$ (Ref. 93 and references cited therein). For evaporation a "microscopic reversibility" is introduced but the resulting factor α for evaporation may differ from the α for condensation, except at equilibrium. The α for condensation of a purely monatomic species is about 1.0.⁹⁶ The α for evaporation of forsterite is temperature dependent and varying between 0.04 and 0.17 in the presence and absence of H_2 (data are summarized in Ref. 99). A value of α for condensation of forsterite has also been obtained and is approximately equal to that for evaporation.¹⁰⁰

This evaporation of Mg_2SiO_4 in the presence of H_2 involves the inverse of the two reactions in Eq. (16), and we infer from Ref. 99 that α is more or less similar for these two

reactions. We can then use the HKS formalism, together with the data in Ref. 93, to conclude that H_2O is favored over O in Eq. (16) as the dominant reactant in the condensation. This result is due to the ratio of the gas phase concentrations $\text{H}_2\text{O}/\text{O}$ being very large,¹⁰¹ $\sim 1.5 \times 10^3$ at 2000 K and much larger at 1500 K.

The equilibrium condensation temperature for Mg_2SiO_4 has been calculated to occur somewhat below 1500 K,⁴⁷ though the kinetic factor will raise that value. The latter has been suggested¹⁰² as a possible reason for Mg_2SiO_4 being more refractory than expected from equilibrium calculations. Dust enrichment also raises the condensation temperature.⁴⁴

In the case of Ca and Al minerals, the Ca and Al concentrations are the smallest ones in the condensing species and in a HKS analysis will typically be rate controlling, i.e., the rate will be proportional to $(\text{Ca}-\text{Ca}^e)$, where Ca^e is the equilibrium concentration determined from the HKS formalism.⁹⁵

III. DISCUSSION

The slope of a three-isotope enrichment plot of $^{17}\text{O}/^{16}\text{O}$ versus $^{18}\text{O}/^{16}\text{O}$ need not be exactly 1.0 to be described as mass independent. For example, in the case of ozone the enrichments of the many isotopologues for heavily ^{17}O and ^{18}O enriched systems are not exactly equal, either experimentally⁷³ or theoretically.^{62,63} There are very small mass-dependent contributions.⁸⁷ However, on theoretical grounds such differences are expected to disappear at high temperatures, thus making the plot of $\delta^{17}\text{O}$ versus $\delta^{18}\text{O}$ for CAIs formed at high temperatures have a slope close to 1.0. For the CAIs from the Allende meteorite, the slope of the line is 0.94 ± 0.02 .²¹ However, it has been argued that when corrected for some subsequent processing, the slope is 1.0.¹²

Other reactions also show interesting isotopic mass anomalies. The reaction $\text{CO} + \text{OH} \rightarrow \text{CO}_2 + \text{H}$ has a $\Delta^{17}\text{O}$, defined as $\delta^{18}\text{O} - 0.52\delta^{17}\text{O}$, which differs from the mass-dependent value of zero and so is anomalous.^{101,103,104} Data^{101,103} for a plot of $\delta^{18}\text{O}$ versus $\delta^{17}\text{O}$ are presently too few to determine the slope unequivocally, but a preliminary value is about 0.7–0.75.⁸² There is some reason, therefore, to suspect that it may not produce the desired slope of 1.0, or very close to 1.0, found for the CAIs. Again, a mass anomaly in the O isotopic composition in CO in the atmosphere has been attributed to the $\text{CO} + \text{OH}$ reaction and the data show a slope less than 0.52.¹⁰⁵ Indeed, unlike the phenomenon in ozone, no theoretical argument has been offered thus far to suggest that this reaction should show a slope of unity. At the moment, therefore, if there is a chemical origin for the mass-independent isotope phenomenon in CAIs, we appear to be left with an origin based on the η effect in transient surface recombination.

Any quantitative theory for the η effect will involve detailed quantum mechanical calculations on the formation, lifetime, and disappearance of vibrationally excited chemical intermediates. Such calculations are computationally intensive and are now being undertaken for ozone.^{106,107} The results will be extremely interesting. It will be an added challenge to calculate δQ , since it is a small difference between four large quantities.⁶⁰

When the η effect is intramolecular based (the first origin listed in Appendix A) one expects that the magnitude of η will depend on the density of states, ρ , of the vibrationally excited molecule: When the states are sparse, i.e., when ρ is small, there will be less efficient intramolecular energy transfer and so less “statistical” behavior. Intramolecular energy transfer occurs by internal resonances among the various coordinates, and the probability of these resonances existing is smaller when ρ is smaller.

Ozone has a relatively low dissociation energy of about 1.1 eV, and so ρ is comparatively small. The dissociation energies of SiO_2 and AlO_2 are larger. As a result, they have a higher ρ , and so may be less apt to show nonstatistical behavior. On the other hand, in the limited data available covering a 200 K range in temperature, the η for ozone increased with increasing temperature.⁷⁰ This effect can be understood or rationalized in terms of either mechanism and is related to a shorter time for energy redistribution or for collisional deactivation energy transfer at the prevailing pressure when the temperature is increased. Thus, the η effect may be larger at the high temperatures of 1500–2000 K.

To obtain a δQ of -40 per mil in the present case, using a typical w of $1/2$ in Eq. (12), an R of about 1.08 is needed. In the present case a δQ of 1.04 corresponds to an R of 1.08 and to an η of 1.08. In the case of ozone, η was about 1.15 and corresponded to an R of about 1.10.¹⁰⁸ There is no reason why the two η 's, obtained at very different temperatures and for very different molecules, should be the same, but a lower η for the CAIs can arise from the deactivation in Eq. (8). In the case of ozone the enrichment is temperature dependent. It increases with increasing temperature,⁷⁰ and hence η also does.

The magnitude of R at 1500–2000 K in Eq. (10) has not been experimentally measured for the CAIs, or for any reaction, gas or surface-based, at those temperatures. Experiments on the isotope effect on the gas recombination phase reaction $\text{O} + \text{XO} + \text{M} \rightarrow \text{XO}_2 + \text{M}$ at low pressures (M is a third body) and high temperatures, with $X = \text{C}$ or Si , would be useful to see if a nonzero η effect occurs under those conditions. The reaction $\text{O} + \text{CO} + \text{M} \rightarrow \text{CO}_2 + \text{M}$ has been shown to have an anomalous isotope effect at room temperature.¹⁰⁵ It would be interesting to study this reaction at 1500–2000 K, perhaps using N_2O photolysis as a source of O. (Use of O_2 photolysis has added complications, due to the transient O_3 formed. Use of N_2O is also complicated since it yields $\text{O}(^1\text{D})$ atoms, depending upon the wavelength.) The $\text{O} + \text{CO}$ reaction can have an anomalous ^{18}O effect, due to an η effect. A twofold effect may occur for ^{17}O , due to an η effect and a possible hyperfine spin–spin interaction, since ^{17}O has a nuclear spin and so the spin-forbidden nature of the reaction may be less (Appendix F).

The more difficult study of the existence of an η effect on a solid phase (or melt) would be particularly desirable, using a source of SiO and of H_2O (or O), and other atoms such as Ca or Al. The latter would also provide nearby electron spins which would reduce the spin-forbidden nature of reaction (1) (Appendix F). The conditions need to be such as to favor an $\text{XO}_{\text{ads}} + \text{O}_{\text{ads}} \rightleftharpoons \text{XO}_{2\text{ads}}^*$ equilibrium on the surface, with the removal of the deactivated ^{17}O - and ^{18}O -rich

XO_2 , as in Fig. 1, instead of its remaining permanently on the surface.

This removal of the ^{17}O - and ^{18}O -rich SiO_2 from the surface of the growing CAI may be by evaporation, as in Fig. 1, or by reaction with H. In this view a reducing atmosphere, perhaps similar to that in solar gas, may be helpful. Whether well-defined crystallization processes (e.g., methods of vapor phase crystal growth discussed in Refs. 109 and 110) are needed is not clear. However, an interesting result has been obtained, in which a “smoke” of composition $\text{SiO}_{1.5}$ - $\text{SiO}_{1.8}$ was produced from silanes, oxygen, and hydrogen in a condensation flow apparatus.⁷⁹ Two of the three experiments yielded mass-dependent results for a $\delta^{17}\text{O}$ versus $\delta^{18}\text{O}$. However, one experiment which was abbreviated abruptly by an explosion¹¹¹ gave anomalous isotopic results, the solids being richer in ^{16}O than in the starting material and with an anomalous slope of 0.72 for the $\delta^{17}\text{O}$ versus $\delta^{18}\text{O}$ plot.

Whether or not the shorter available time for isotopic equilibration was a factor or whether at the relatively low temperature (800 K) and in an environment relatively oxidizing compared with solar gas the observed effect was volume based rather than surface-based remains to be investigated. The absence of an extra enhancement of $\delta^{17}\text{O}$ due to hyperfine interaction (Appendix F) in this metal atom-free (but not spin free) system is of interest. While the ground state of O is a triplet, and so reactions (4)–(6) are spin forbidden when they occur in the gas phase, the spin state of O_{ads} remains to be clarified.

To form ferromagnesian silicates with an artificially high ^{16}O content in this type of laboratory experiment, even though they are not normally so ^{16}O rich, the starting laboratory material could contain Fe and Mg in small amounts relative to the silica together with a quantity of more volatile metals, and no Ca and Al. Use of the same conditions as for the CAIs, but at a lower temperature to permit deposition, will lead to heavily ^{16}O enriched ferromagnesian silicates, if the present surface-based mechanism is applicable. The enrichment would be mass independent.

ACKNOWLEDGMENTS

It is a pleasure to acknowledge the support of this research by the National Science Foundation. The many interactions with Wei-Chen Chen have been invaluable. I am pleased to acknowledge earlier discussions with my other co-workers, Dr. Y. Q. Gao and Dr. J. Weibel. It is particularly a pleasure, too, to acknowledge helpful discussions and correspondence with many colleagues—Dr. C. Alexander, Dr. R. Clayton, Dr. J. R. Lyons, Dr. K. D. McKeegan, Dr. A. Pack, Dr. H. Palme, Dr. M. H. Thiemens, Dr. E. D. Young, and Dr. G. J. Wasserburg. I am pleased to acknowledge the many discussions with members of the Institute of Geophysical and Planetary Physics at UCLA while I was a guest and Slichter Lecturer at that Institute.

APPENDIX A: NATURE OF THE η EFFECT

We briefly summarize here the nature of the η effect. There are two possible origins, intramolecular and intermolecular.⁶³ We consider the intramolecular origin first.

If Q denotes ^{17}O or ^{18}O , in an intramolecular η effect the vibrationally excited asymmetric molecule $\text{OX}Q^*$ formed from $\text{OX}+Q$ or $\text{O}+QX$ has more mixing of vibrational energy among its various vibrational modes than has a symmetric molecule OXO^* formed from $\text{O}+\text{XO}$: There is more mixing because some of the Hamiltonian terms (the dynamical matrix elements responsible for the mixing) are forbidden by symmetry in OXO^* , but not in $\text{OX}Q^*$. The poorer mixing yields a less statistical behavior and, thereby, a smaller effective density of quantum states of the vibrationally excited molecule and, in RRKM-type theory, a longer lifetime for dissociation. Its longer life makes it more likely to be deactivated by collision to form $\text{OX}Q$ than does OXO , and so yields a higher recombination rate constant. This recombination rate constant is mass independent since the asymmetry property and its consequence noted above are independent of whether Q is ^{17}O or ^{18}O .^{60–64} Similarly, starting instead from the dioxide, one can show that the thermal dissociation rate constant for $\text{OX}Q$ is mass independently greater than that for a symmetric molecule OXO . There are small mass-dependent terms, whose calculated small magnitude can be seen rather dramatically in Fig. 7 of Ref. 63, where the small boxes represent the size of the mass-dependent effects.

An alternative possible origin of the η effect is an intermolecular one. The density of states in $\text{OO}Q^*$ is twice as large as that in $\text{O}Q\text{O}^*$ or O_3^* and so it has a better chance for collisional energy transfer in the deactivation to form $\text{OO}Q$ or O_3 . There is also a rotational asymmetry in the interaction potential for $\text{OO}Q^*$, but it would be larger for ^{18}O than for ^{17}O and arises from the rotational asymmetry of $\text{OX}Q$ affecting its collisional deactivational energy transfer, as discussed in Ref. 63.

A theoretical expression incorporating the η effect for ozone⁶⁰ is simple looking. It is the analog of Eqs. (9) and (10) and is valid only when there is extensive isotopic exchange. Not realizing this major theoretical proviso, some ozone data have been corrected for isotopic exchange.^{58,70} It should be stressed that it is only the uncorrected data for which current theory yields mass independence,⁶⁰ not the corrected data. Indeed, the key role played by isotopic exchange in achieving the phenomenon of mass independence is evident: when isotopic exchange is deliberately inhibited, strikingly large O isotopic mass effects occur^{66–69} and they are decidedly not mass independent. In the theoretical expression for the enrichment given in Ref. 60 there is an exact cancellation of a mass dependence of the individual rate constants. The cancellation results from a sum of partitioning factors in Ref. 60 being unity when isotopic exchange between atoms and diatomics is complete. It is the partitioning factors that account for individual rate constant ratios having a marked mass dependence observed experimentally. These partitioning factors differ from a statistical value of 1/2 only because of differences in the zero-point energies in the two exit channels of a dissociating $\text{OO}Q^*$ molecule, $\text{OO}Q^* \rightarrow \text{OO}+Q$ and $\text{OO}Q^* \rightarrow \text{O}+\text{O}Q$.

It has been proposed⁷⁰ that the temperature effect in the mass-independent enrichment in ozone has its origin in the $\text{OO}Q^*$'s whose energy is low enough that the differences in

zero-point energies of the two exit channels are important. However, as noted above, in the framework of the theory in Refs. 60–64, the effect of a zero-point energy difference cancels exactly when there is extensive isotopic exchange. So the temperature effect on enrichment has a quite different origin, perhaps the one suggested above.

An interesting feature of the theory and of the two different types of experiments that have been undertaken for ozone formation is that one type (labeled “scrambled”⁶⁰) exhibits mass independence and is independent of the zero-point energy difference effect. It depends only on the η effect. The other type (labeled “unscrambled”⁶⁰) involves ratios of rate constants and is much less sensitive to η . It depends, instead, primarily on the difference in zero-point energies of the two exit channels. It is dependent on the latter because of their effect on the “partitioning factors.” The energy range for the relevant partitioning factors, in turn, depends on a collisional energy transfer term, ΔE .^{62–64} Thus, η affects the scrambled enrichments experiment while ΔE is the dominant factor affecting the individual mass-sensitive ratios of recombination rate constants.

The isotopic exchange also serves to erase any isotopic fractionation resulting from the primary photochemical act, which creates the O atoms that later combine with the O₂ to form O₃. Such fractionation would occur unless the light source is broad enough to encompass the entire absorption band, or happens to occur at the maximum of the absorption band. At wavelengths away from the maximum there are many examples of photolytic fractionation for spin-allowed systems, such as, Ref. 112. When the photolysis is spin forbidden (Appendix F) fractionation occurs at every wavelength.

APPENDIX B: RATES OF O+H₂→OH+H AND O+CO+M→CO₂+M

At 2000 K, the O+H₂ reaction has a rate constant available in standard NIST tables¹¹³ of about 10^{-11} cm³ molecule⁻¹ s⁻¹, and the recombination reaction O+CO+M→CO₂+M, where M is a third body, has a rate constant of about 10^{-33} cm⁶ molecule⁻² s⁻¹. At a pressure of 0.001 bar, its effective bimolecular rate constant is then about 4×10^{-18} cm³ molecule⁻¹ s⁻¹. The ratio of H₂/CO in the solar gas is about 10³. Thus, the ratio of the rate of the O+H₂→OH+H reaction to that of O+CO+M→CO₂+M is about 2.5×10^9 . The ratio of the O+H₂→OH+H reaction rate to that of O+SiO+M→SiO₂+M would be expected to be roughly similar. The lifetime of an O reacting with H₂ is estimated from the rate constant and H₂ concentration in solar gas to be about 25 μs. If the system were dust enriched by a factor of 10³, resulting in a smaller reduced H₂ concentration at the given total pressure, the ratio of rates of reaction of O with H₂ to that with CO would be reduced to 2.5×10^6 , which is still extremely large. Thus, the disappearance of O by three-body recombination is minor under such conditions. The system clearly differs in a major way from the ozone system.

At 1500 K, the O+CO+M→CO₂+M reaction has an effective bimolecular rate constant of 3×10^{-8} cm³ molecule⁻¹ s⁻¹ at 0.001 bar.¹¹³ The O+H₂→OH+H

rate constant is¹¹³ 2.5×10^{-12} cm³ molecule⁻¹ s⁻¹. With a H₂/CO ratio of 1000, the H₂ reaction is faster than CO reaction by a factor of 10⁶.

APPENDIX C: RATE OF H+XO₂→HO+XO, X=C, Si

At 2000 K and 0.001 bar, the rate constant for the reaction H+XO₂→HO+XO, obtained from standard NIST tables¹¹³ for the given conditions, is 3×10^{-13} cm³ molecule⁻¹ s⁻¹ for X=C. Using these tables for the reverse reaction for X=Si and the Janaf Thermodynamic tables,⁸² the rate constant for X=Si is 3×10^{-11} cm³ molecule⁻¹ s⁻¹. For a concentration of H, for the cited conditions, of $\sim 2 \times 10^{14}$ molecule cm⁻³,⁸⁵ the lifetime of a CO₂ molecule is ~ 15 ms and that of a SiO₂ is ~ 150 μs. At 1500 K, the lifetimes are estimated to be longer by a factor of the order of 10.

APPENDIX D: GROWTH RATES AND COMPETITION WITH OTHER SOURCE OF O-ATOM REMOVAL

For concreteness, we consider a stage of growth where 1% of the silicon species is present as grains of radius ~ 100 Å, a radius taken from an interstellar grain size.¹¹⁴ We also consider a radius ~ 1000 Å. Using forsterite, Mg₂SiO₄, as an example, with its known specific gravity, and using the solar elemental abundance,^{84,85} there are calculated to be about 4×10^6 grains cm⁻³ at the temperature and pressure used here. We use the Knudsen-Hertz formula^{96–98} for the rate of condensation on the surface of a grain, $\alpha A c_v (kT/2\pi m)$, with terms defined in the text and with A being the area of the grain. Taking α to be ~ 0.1 (Ref. 93) and using the solar gas concentration of O of $\sim 2 \times 10^8$ cm⁻³ under the cited conditions,⁸² the first-order rate of loss of O onto one grain is calculated to be ~ 75 s⁻¹.

With the above estimate of the grain density, the rate of loss of O on the grains is 3×10^8 atoms cm⁻³ s⁻¹. This quantity is small compared with the rate of loss of O by the reaction O+H₂→OH+H of $\sim 10^{13}$ atom cm⁻³ s⁻¹. So the deposition is indeed a small perturbation of the steady-state O concentration, as would be needed for Eqs. (9) and (10) had O been the dominant reactant in reaction (16) rather than H₂O. For this size grains and pressures, it is also readily shown, by many orders of magnitude, that diffusion in the gas phase to a grain is not the slow step. In the case of H₂O instead of O in reaction (16) yielding O_{ads}, the question of depletion of a steady-state O concentration does not arise.

To consume as much as $\sim 5\%$ of the Si species by forming minerals at the above condensation rate and noting that one SiO disappears for every 20 O atoms, the rate of loss of the SiO is twice as great as that of the O atoms, and so is of the order of 1.5×10^8 molecule cm⁻³. Since there are $\sim 3 \times 10^{11}$ SiO cm⁻³ initially, one would require a time $\sim 3 \times 10^{11}/(20)(1.5) \times 10^8$, i.e., $\sim 10^2$ s, a very short time. As the particles grow, the surface/volume ratio decreases, and the rate of deposition of SiO becomes slower, but not dramatically. We also see that there is no need to postulate a photochemical source of O to reduce the time of the O deposition. At 1500 K, the AlO and SiO concentrations are about the same as at 2000 K, but the O concentration is about a

factor of 2.5×10^4 less, so there is lengthening of time for 5% deposition of O to $\sim 2.5 \times 10^6$ s, which is still a very short time.

The O atom concentration was estimated as $\sim 2 \times 10^8$ atom cm^{-3} , but other atoms or groups must also deposit on the surface to form CAIs: Al, Ca, and AlO have concentrations which are 35, 20, and 1/12 of the O concentration, and so when AlO is involved the deposition time would be somewhat slower by perhaps a factor of 10.

If, instead, a radius of 1000 Å had been assumed for the dust particles, with the same conversion of 1% of the Si to dust, the total number of grains would have been 1000-fold less, but the area of each would have been 100-fold more. Thus, the total grain area per unit volume of the gas would have been tenfold less, and the process to form 5% solids would have taken longer by a factor of 10, which is still a short time.

APPENDIX E: RATE OF $\text{OH} + \text{H}_2 \rightarrow \text{H}_2\text{O} + \text{H}$, $\text{OH} + \text{H} \rightarrow \text{O} + \text{H}_2$ AND LIFETIME OF OH

At 2000 K and 0.001 bar, the OH can disappear by $\text{OH} + \text{H}_2 \rightarrow \text{H}_2\text{O} + \text{H}$, whose rate constant k_1 in standard NIST tables¹¹³ is $\sim 9 \times 10^{-12} \text{ cm}^3 \text{ molecule}^{-1} \text{ s}^{-1}$. For the three-body reaction $\text{OH} + \text{H} + M \rightarrow \text{H}_2\text{O} + M$ (same tables), the rate constant is $\sim 1.5 \times 10^{-32} \text{ cm}^6 \text{ molecule}^{-2} \text{ s}^{-1}$. At the prevailing pressure and H_2/H ratio, one finds that it is a factor of 3×10^6 slower than the reaction with H_2 . The k_1 given above, multiplied by the H_2 concentration of $4 \times 10^{15} \text{ molecule cm}^{-3}$, yields a lifetime of OH of the order of 30 μs . At 1500 K the lifetime of OH in the $\text{OH} + \text{H} \rightarrow \text{H} + \text{H}_2\text{O}$ reaction is estimated from Ref. 113 to be 60 μs .

The rate constant for $\text{OH} + \text{H} \rightarrow \text{O} + \text{H}_2$, obtained from NIST tables,¹¹³ is $\sim 5 \times 10^{-12} \text{ cm}^3 \text{ molecule}^{-1} \text{ s}^{-1}$. With a concentration of H of $\sim 2 \times 10^{14} \text{ atoms cm}^{-3}$, the probability that an OH will undergo this reaction is 10^3 s^{-1} and so its lifetime with respect to this reaction is 1 ms.

APPENDIX F: SPIN-FORBIDDEN REACTIONS AND REDUCTION OF "FORBIDDENNESS"

An example of a spin-forbidden transition is the photolysis from a ground state singlet to an electronically excited triplet state of the dioxide, e.g., of CO_2 or SiO_2 . This process has been shown for CO_2 to favor ^{17}O production, because the electron spin-nuclear spin coupling ("hyperfine interaction") reduces the "spin forbiddenness".¹¹⁵ The ^{17}O has a nuclear spin but the ^{16}O and the ^{18}O do not.

¹J. H. Chen and G. J. Wasserburg, *Earth Planet. Sci. Lett.* **52**, 1 (1981).

²A. W. Hsu, G. J. Wasserburg, and G. R. Huss, *Earth Planet. Sci. Lett.* **182**, 15 (2000).

³M. Wadhwa and S. S. Russell, in *Protostars and Planets IV*, edited by V. Mannings, A. P. Boss, and S. S. Russell (University of Arizona Press, Tucson, 2000), pp. 995–1018.

⁴C. Allegre, *Philos. Trans. R. Soc. London, Ser. A* **359**, 2137 (2001).

⁵Y. Guan, G. R. Huss, G. L. MacPherson, and G. J. Wasserburg, *Science* **289**, 1330 (2000).

⁶R. N. Clayton, L. Grossman, and T. K. Mayeda, *Science* **182**, 485 (1973).

⁷A. N. Krot, K. D. McKeegan, L. A. Leshin, G. J. MacPherson, and E. R. D. Scott, *Science* **295**, 1051 (2002).

⁸E. R. D. Scott and A. N. Krot, *Meteorit. Planet. Sci.* **36**, 1307 (2001).

⁹L. A. Leshin, A. E. Rubin, and K. D. McKeegan, *Geochim. Cosmochim. Acta* **61**, 835 (1997).

¹⁰R. N. Clayton and T. K. Mayeda, *Geochim. Cosmochim. Acta* **63**, 2089 (1999).

¹¹A. E. Rubin, J. T. Wasson, R. N. Clayton, and T. K. Mayeda, *Earth Planet. Sci. Lett.* **96**, 247 (1989).

¹²E. D. Young and S. S. Russell, *Science* **282**, 452 (1998).

¹³C. Engrand, K. D. McKeegan, and L. A. Leshin, *Geochim. Cosmochim. Acta* **63**, 2623 (1999).

¹⁴Y. Guan, K. D. McKeegan, and G. J. MacPherson, *Earth Planet. Sci. Lett.* **181**, 271 (2000).

¹⁵S. S. Russell, G. J. MacPherson, L. A. Leshin, and K. D. McKeegan, *Earth Planet. Sci. Lett.* **184**, 576 (2000).

¹⁶K. D. McKeegan, L. A. Leshin, S. S. Russell, and G. J. MacPherson, *Science* **280**, 414 (1998).

¹⁷T. J. Fagan, K. D. McKeegan, A. N. Krot, and K. Keil, *Meteorit. Planet. Sci.* **36**, 223 (2001).

¹⁸H. Hiyagon and A. Hashimoto, *Science* **282**, 828 (1999).

¹⁹R. N. Clayton, *Annu. Rev. Earth Planet Sci.* **21**, 115 (1993).

²⁰H. Yurimoto, M. Ito, and H. Nagasawa, *Science* **282**, 1874 (1998).

²¹R. N. Clayton, N. Onuma, L. Grossman, and T. K. Mayeda, *Earth Planet. Sci. Lett.* **34**, 209 (1977).

²²H. Nagahara, *Meteorit. Planet. Sci.* **36**, 1011 (2001).

²³P. Cassen, *Philos. Trans. R. Soc. London, Ser. A* **359**, 1935 (2001).

²⁴C. M. O. D. Alexander, A. P. Boss, and R. W. Carlson, *Science* **293**, 64 (2001).

²⁵A. N. Krot, A. Meibom, S. S. Russell, C. M. O. D. Alexander, T. E. Jeffries, and K. Keil, *Science* **291**, 1776 (2001).

²⁶D. Wark and W. V. Boynton, *Meteorit. Planet. Sci.* **36**, 1135 (2001).

²⁷S. S. Russell, G. R. Huss, A. J. Fahey, R. C. Greenwood, R. Hutchison, and G. J. Wasserburg, *Geochim. Cosmochim. Acta* **62**, 689 (1998).

²⁸H. Palme, *Philos. Trans. R. Soc. London, Ser. A* **359**, 2061 (2001).

²⁹A. P. Boss, *Annu. Rev. Earth Planet Sci.* **26**, 53 (1998).

³⁰A. Ruzicka, *J. Geophys. Res.* **102**, 13387 (1997).

³¹A. P. Boss, in *Chondrules and the Protoplanetary Disk*, edited by R. H. Hewins, Q. H. Jones, and E. R. D. Scott (Cambridge University Press, Cambridge, 1996), pp. 257–263.

³²F. H. Shu, H. Shang, M. Gounelle, A. E. Glassgold, and T. Lee, *Astrophys. J.* **548**, 1029 (2001).

³³H. Palme and W. V. Boynton, in *Protostars and Planets III*, edited by E. H. Levy and J. I. Lunine (University of Arizona Press, Tucson, 1993), pp. 979–1004.

³⁴L. Grossman and J. W. Larimer, *Rev. Geophys. Space Phys.* **12**, 71 (1974).

³⁵G. J. MacPherson, D. A. Wark, and J. T. Armstrong, in *Meteorites and the Early Star System*, edited by J. F. Kerridge and M. S. Mathews (University of Arizona Press, Tucson, 1988), pp. 746–807.

³⁶H. Y. McSween, *Meteoritics* **20**, 523 (1985).

³⁷A. M. Davis and G. J. MacPherson, in *Chondrules and the Protoplanetary Disk*, edited by Q. H. Hewins, R. H. Jones, and E. R. D. Scott (Cambridge University Press, Cambridge, 1996), pp. 71–76.

³⁸A. N. Krot and K. Keil, *Meteorit. Planet. Sci.* **37**, 91 (2002).

³⁹E. R. D. Scott, S. G. Love, and A. N. Krot, in *Chondrules and the Protoplanetary Disk*, edited by R. H. Hewins, R. H. Jones, and E. R. D. Scott (Cambridge University Press, Cambridge, 1996), pp. 87–96.

⁴⁰J. W. Larimer, J. T. Wasson, G. J. MacPherson, D. A. Wark, and J. T. Armstrong, in *Meteorites and the Early Star System*, edited by J. F. Kerridge and M. S. Mathews (University of Arizona Press, Tucson, 1988), pp. 395–415.

⁴¹R. H. Jones, T. Lee, H. C. Connolly, S. G. Love, and H. Shang, in *Protostars and Planets IV*, edited by V. Mannings, A. P. Boss, and S. S. Russell (University of Arizona Press, Tucson, 2000), pp. 927–961.

⁴²A. E. Rubin, B. Fegley, and R. Brett, in *Meteorites in the Early Solar System*, edited by J. F. Kerridge and M. S. Mathews (University of Arizona Press, Tucson, 1988), pp. 488–511.

⁴³A. N. Krot, B. Fegley, K. Lodders, and H. Palme, in *Protostars and Planets IV*, edited by V. Mannings, A. P. Boss, and S. S. Russell (University of Arizona Press, Tucson, 2000), pp. 1019–1054.

⁴⁴D. S. Ebel and L. Grossman, *Geochim. Cosmochim. Acta* **64**, 339 (2000).

⁴⁵L. Grossman, D. S. Ebel, S. B. Simon, A. M. Davis, F. M. Richter, and N. M. Parsad, *Geochim. Cosmochim. Acta* **64**, 2879 (2000).

⁴⁶J. A. Wood and A. Hashimoto, *Geochim. Cosmochim. Acta* **57**, 2887 (1993).

⁴⁷S. Yoneda and L. Grossman, *Geochim. Cosmochim. Acta* **59**, 3413 (1995).

⁴⁸O. Navon and G. J. Wasserburg, *Earth Planet. Sci. Lett.* **73**, 1 (1985).

- ⁴⁹R. N. Clayton, *Nature (London)* **415**, 860 (2002).
- ⁵⁰M. H. Thiemens, *Science* **219**, 1073 (1983).
- ⁵¹M. H. Thiemens, in *Chondrules and the Protoplanetary Disk*, edited by R. H. Hewins, R. H. Jones, and E. R. D. Scott (Cambridge University Press, Cambridge, 1996), pp. 107–118.
- ⁵²D. D. Clayton, *Astrophys. J.* **334**, 191 (1988).
- ⁵³K. D. McKeegan (private communication).
- ⁵⁴J. R. Lyons and E. D. Young, *Proceedings of XXXIV Lunar and Planetary Science Conference*, Abstract 1981, 2003.
- ⁵⁵J. E. Heidenreich and M. H. Thiemens, *J. Chem. Phys.* **78**, 892 (1983).
- ⁵⁶M. H. Thiemens, *Science* **283**, 341 (1999).
- ⁵⁷R. E. Weston, *Chem. Rev. (Washington, D.C.)* **99**, 2115 (1999).
- ⁵⁸K. Mauersberger, D. Krankowsky, C. Janssen, and R. Schinke, *Adv. At. Mol. Opt. Phys.* (to be published).
- ⁵⁹J. Yang and S. Epstein, *Geochim. Cosmochim. Acta* **51**, 2011 (1987).
- ⁶⁰B. C. Hathorn and R. A. Marcus, *J. Chem. Phys.* **111**, 4087 (1999).
- ⁶¹B. C. Hathorn and R. A. Marcus, *J. Chem. Phys.* **113**, 9497 (2000).
- ⁶²Y. Q. Gao and R. A. Marcus, *Science* **293**, 259 (2001).
- ⁶³Y. Q. Gao and R. A. Marcus, *J. Chem. Phys.* **116**, 137 (2002).
- ⁶⁴Y. Q. Gao, W. C. Chen, and R. A. Marcus, *J. Chem. Phys.* **117**, 1536 (2002).
- ⁶⁵S. M. Anderson, D. Huelsebush, and K. Mauersberger, *J. Chem. Phys.* **107**, 5385 (1998).
- ⁶⁶J. Güenther, B. Erbacher, D. Krankowsky, and K. Mauersberger, *Chem. Phys. Lett.* **306**, 209 (1999).
- ⁶⁷C. Janssen, J. Güenther, D. Krankowsky, and K. Mauersberger, *J. Chem. Phys.* **111**, 7179 (1999).
- ⁶⁸J. Güenther, D. Krankowsky, and K. Mauersberger, *Chem. Phys. Lett.* **324**, 31 (2000).
- ⁶⁹M. H. Thiemens and T. Jackson, *Geophys. Res. Lett.* **17**, 717 (1990).
- ⁷⁰J. Morton, J. Barnes, B. Schueler, and K. Mauersberger, *J. Geophys. Res.* **95**, 901 (1990).
- ⁷¹J. Morton, B. Schueler, and K. Mauersberger, *Chem. Phys. Lett.* **154**, 143 (1989).
- ⁷²K. Mauersberger, *Geophys. Res. Lett.* **14**, 80 (1987).
- ⁷³K. Mauersberger, J. Morton, B. Schueler, J. Stehr, and S. M. Anderson, *Geophys. Res. Lett.* **20**, 1031 (1993).
- ⁷⁴D. Krankowsky and K. Mauersberger, *Science* **274**, 1324 (1996).
- ⁷⁵K. Mauersberger, B. Erbacher, D. Krankowsky, J. Güenther, and R. Nickel, *Science* **283**, 370 (1999).
- ⁷⁶E. Stolper, *Geochim. Cosmochim. Acta* **46**, 2159 (1982).
- ⁷⁷J. R. Beckett and E. Stolper, *Meteoritics* **29**, 41 (1994).
- ⁷⁸F. Robert, Second International Symposium on Isotopomers (ISI) Stresa, Italy, 4–7 Nov. 2003.
- ⁷⁹M. H. Thiemens, R. Nelson, and Q. W. Ding, *Proceedings of the XXV Lunar and Planetary Science Conference*, Abstract 1398, 1994.
- ⁸⁰R. Nelson, M. Thiemens, J. Nuth, and B. Donn, *Proceedings of the XIX Lunar Planetary Science Conference*, Abstract 559, 1989.
- ⁸¹M. Slack and A. Grillo, *Combust. Flame* **59**, 189 (1985).
- ⁸²W. C. Chen and R. A. Marcus (unpublished). Thermodynamic results were largely obtained from Janaf Thermodynamic Tables <http://webbook.nist.gov/chemistry/form-ser.html> using solar abundances in Refs. 84 and 85. In some cases, such as for Si(OH)₂ the results were supplemented by electronic structure calculations.
- ⁸³G. Vidali, J. E. Roser, G. Manico, and V. Pirronello, *Adv. Space Res.* **33**, 6 (2004).
- ⁸⁴K. Lodders, *Astrophys. J.* **591**, 1220 (2003).
- ⁸⁵E. Anders and N. Grevesse, *Geochim. Cosmochim. Acta* **53**, 197 (1989).
- ⁸⁶R. H. Nichols, R. T. Grimaldi, and G. J. Wasserburg, *Meteorit. Planet. Sci.* **33**, A155 (1998).
- ⁸⁷The smallness of those contributions is seen from the small heights of the white boxes in Fig. 7 in Ref. 63 for isotopologues which are not purely symmetric and from 1/3 the height of the boxes for the purely symmetric species OOO and QQQ.
- ⁸⁸A. E. Nielsen, *Pure Appl. Chem.* **53**, 2025 (1981).
- ⁸⁹A. E. Nielsen, *J. Cryst. Growth* **67**, 289 (1984).
- ⁹⁰P. P. Chang and M. D. Donahue, *J. Colloid Interface Sci.* **122**, 230 (1988).
- ⁹¹W. K. Burton, N. Cabrera, and F. C. Frank, *Proc. R. Soc. London* **B243**, 299 (1951).
- ⁹²J. Zhang and G. H. Nancollas, *J. Colloid Interface Sci.* **200**, 131 (1998).
- ⁹³A. Tsuchiyama, S. Tachibana, and T. Takahashi, *Geochim. Cosmochim. Acta* **63**, 2451 (1999).
- ⁹⁴T. Sata, T. Sasamoto, H. L. Lee, and E. Maeda, *Rev. Int. Haates Temp. Refract.* **15**, 237 (1978).
- ⁹⁵R. A. Marcus (unpublished).
- ⁹⁶J. P. Hirth and G. M. Pound, in *Condensation and Evaporation, Nucleation and Growth Kinetics* (Pergamon, Oxford, 1963), pp. 123–124.
- ⁹⁷H. Hertz, *Ann. Phys. (Leipzig)* **17**, 193 (1882).
- ⁹⁸M. Knudsen, *Ann. Phys. (Leipzig)* **47**, 697 (1915).
- ⁹⁹A. Tsuchiyama, T. Takahashi, and S. Tachibana, *Mineral. J.* **20**, 113 (1998).
- ¹⁰⁰H. Inaba, S. Tachibana, H. Nagahara, and K. Ozawa, *Proceedings of the XXXII Lunar and Planetary Science Conference*, Abstract 1837, 2001.
- ¹⁰¹C. M. Stevens, L. Kaplan, R. Gorse, S. Durkee, M. Compton, S. Cohen, and K. Bielling, *Int. J. Chem. Kinet.* **12**, 935 (1980).
- ¹⁰²A. Hashimoto, *Nature (London)* **347**, 53 (1990).
- ¹⁰³T. Rockmann, C. Brenninkmeijer, G. Saveressig, P. Begmaschi, J. Crowley, H. Fischer, and P. Crutzen, *Science* **281**, 544 (1998).
- ¹⁰⁴A. K. Huff and M. H. Thiemens, *Geophys. Res. Lett.* **25**, 3509 (1998).
- ¹⁰⁵S. K. Bhattacharya and M. H. Thiemens, *Z. Naturforsch. A* **44A**, 811 (1989).
- ¹⁰⁶D. Charlo and D. C. Clary, *J. Chem. Phys.* **120**, 2700 (2004).
- ¹⁰⁷D. Babikov, B. K. Kendrick, R. B. Walker, R. T. Pack, P. Fleurat-Lesard, and R. Schinke, *J. Chem. Phys.* **118**, 6298 (2003), and references cited therein.
- ¹⁰⁸In the ozone system in Refs. 60–64, there are three terms in the equation corresponding to Eq. (10), the third arising from OQO in the ozone. This difference only reduces the result of the η effect. In particular, the η of 1.15 corresponded to an R of $\approx[(1.15)(2/3)+1.0/3]$, i.e., 1.10 or 10 parts per mil.
- ¹⁰⁹G. B. Stringfellow, in *Crystal Growth*, edited by B. R. Pamplin (Pergamon, Oxford, 1980), pp. 181–220.
- ¹¹⁰R. Z. Bachrach, in *Crystal Growth*, edited by B. R. Pamplin (Pergamon, Oxford, 1980), pp. 221–274.
- ¹¹¹M. H. Thiemens (private communication).
- ¹¹²F. Turatti, D. W. T. Griffith, S. R. Wilson, M. B. Esler, T. Rahn, H. Zhang, and G. A. Blake, *Geophys. Res. Lett.* **27**, 2489 (2000).
- ¹¹³See <http://kinetics.nist.gov/index.php>, <http://kinetics.nist.gov/index.php>
- ¹¹⁴B. T. Draine, *Astrophys. J.* **598**, 1026 (2003).
- ¹¹⁵S. E. Bhattacharya, J. Savarino, and M. H. Thiemens, *Geophys. Res. Lett.* **27**, 1459 (2000).